REPORT DOCUMENTATION PAGE

Form Approved
OMB NO. 0704-0188

1. AGENCY USE ONLY (Leave Blank)	2. REPORT DATE 2/25/05	3. REPORT TYPE AND DATES COVERED Reprint

4. TITLE AND SUBTITLE
Equations for finite-difference, time-domain simulation of sound propagation in moving inhomogeneous media and numerical implementation

5. FUNDING NUMBERS
DAAD19-01-1-0640

6. AUTHOR(S)
V.E. Ostashev, D.K. Wilson, L.Liu, D.F. Aldridge, N.P. Symons, and D.H. Marlin

7. PERFORMING ORGANIZATION NAME(S) AND ADDRESS(ES)
Physics Department, New Mexico State University,
Box 30001, Dept. 3D, Las Cruces, NM 88003

8. PERFORMING ORGANIZATION REPORT NUMBER

9. SPONSORING / MONITORING AGENCY NAME(S) AND ADDRESS(ES)
U. S. Army Research Office
P.O. Box 12211
Research Triangle Park, NC 27709-2211

10. SPONSORING / MONITORING AGENCY REPORT NUMBER
42469.24-EV-H

11. SUPPLEMENTARY NOTES
The views, opinions and/or findings contained in this report are those of the author(s) and should not be construed as an official Department of the Army position, policy or decision, unless so designated by other documentation.

12 a. DISTRIBUTION / AVAILABILITY STATEMENT
Approved for public release; distribution unlimited.

12 b. DISTRIBUTION CODE

13. ABSTRACT (Maximum 200 words)
See the reprint attached.

14. SUBJECT TERMS

15. NUMBER OF PAGES
15

16. PRICE CODE

17. SECURITY CLASSIFICATION OR REPORT	18. SECURITY CLASSIFICATION ON THIS PAGE	19. SECURITY CLASSIFICATION OF ABSTRACT	20. LIMITATION OF ABSTRACT
UNCLASSIFIED	**UNCLASSIFIED**	**UNCLASSIFIED**	**UL**

Equations for finite-difference, time-domain simulation of sound propagation in moving inhomogeneous media and numerical implementation[a)]

Vladimir E. Ostashev
NOAA/Environmental Technology Laboratory, Boulder, Colorado 80305, and Department of Physics, New Mexico State University, Las Cruces, New Mexico 88003

D. Keith Wilson and Lanbo Liu
U.S. Army Engineer Research and Development Center, Hanover, New Hampshire 03755

David F. Aldridge and Neill P. Symons
Department of Geophysical Technology, Sandia National Labs., Albuquerque, New Mexico 87185

David Marlin
U.S. Army Research Laboratory, White Sands Missile Range, New Mexico 88002

(Received 24 February 2004; revision received 14 October 2004; accepted 5 November 2004)

Finite-difference, time-domain (FDTD) calculations are typically performed with partial differential equations that are first order in time. Equation sets appropriate for FDTD calculations in a moving inhomogeneous medium (with an emphasis on the atmosphere) are derived and discussed in this paper. Two candidate equation sets, both derived from linearized equations of fluid dynamics, are proposed. The first, which contains three coupled equations for the sound pressure, vector acoustic velocity, and acoustic density, is obtained without any approximations. The second, which contains two coupled equations for the sound pressure and vector acoustic velocity, is derived by ignoring terms proportional to the divergence of the medium velocity and the gradient of the ambient pressure. It is shown that the second set has the same or a wider range of applicability than equations for the sound pressure that have been previously used for analytical and numerical studies of sound propagation in a moving atmosphere. Practical FDTD implementation of the second set of equations is discussed. Results show good agreement with theoretical predictions of the sound pressure due to a point monochromatic source in a uniform, high Mach number flow and with Fast Field Program calculations of sound propagation in a stratified moving atmosphere. © *2005 Acoustical Society of America.* [DOI: 10.1121/1.1841531]

PACS numbers: 43.20.Bi, 43.28.Js [MO] Pages: 503–517

I. INTRODUCTION

Finite-difference, time-domain (FDTD) techniques have drawn substantial interest recently due to their ability to readily handle complicated phenomena in outdoor sound propagation such as scattering from buildings and trees, dynamic turbulence fields, complex moving source distributions, and propagation of transient signals.[1–8] These phenomena are difficult to handle with frequency–domain techniques that are currently widely used, such as parabolic equation approximations and the Fast Field Program (FFP). FDTD techniques typically solve coupled sets of partial differential equations that are first order in time. In this regard, they are a departure from methodologies such as the parabolic approximation, which solve a single equation for the sound pressure that is second order in time. Many such single equations for the sound pressure in a moving inhomogeneous medium are known in the literature (see Refs. 9–14 and references therein). Although these equations were obtained with different assumptions and/or approximations, all contain second- or higher-order derivatives of the sound pressure with respect to time, and are therefore not amenable to first-order FDTD techniques. Our main goal in the present paper is to derive equation sets that are appropriate as starting equations in FDTD simulations of sound propagation in a moving inhomogeneous atmosphere and to study the range of applicability of these sets.

The most general possible approach to sound propagation in a moving inhomogeneous medium would be based on a direct solution of the complete set of linearized equations of fluid dynamics,[9–11,15] which are first-order partial differential equations. Although this set could be used as starting equations for FDTD codes, even with modern computers it is too involved to be practical. Furthermore, this set contains the ambient pressure and entropy, which are not usually considered in studies of sound propagation in the atmosphere. Therefore, it is worthwhile to find simplified equation sets for use in FDTD calculations.

In the present paper, the complete set of linearized equations of fluid dynamics in a moving inhomogeneous medium is reduced to two simpler sets that are first order in time and

[a)]Portions of this work were presented in V. E. Ostashev, L. Liu, D. K. Wilson, M. L. Moran, D. F. Aldridge, and D. Marlin, "Starting equations for direct numerical simulation of sound propagation in the atmosphere," *Proceedings of the 10th International Symposium on Long Range Sound Propagation*, Grenoble, France, Sept. 2002, pp. 73–81.

amenable to FDTD implementation. The first set contains three coupled equations involving the sound pressure, vector acoustic (particle) velocity, and acoustic density. No approximations are made in deriving this set. The second set contains two coupled equations for the sound pressure and vector acoustic velocity. Although the second set describes sound propagation only approximately, the assumptions involved in deriving the second set are quite reasonable in atmospheric acoustics: Terms proportional to the divergence of the medium velocity and the gradient of the ambient atmospheric pressure are ignored. To better understand the range of applicability of the second set, we compare the set with equations for the sound pressure that have been previously used in analytical and numerical studies of sound propagation in a moving atmosphere. It is shown that the second set has the same or a wider range of applicability than these equations for the sound pressure.

Furthermore in the present paper, a basic numerical algorithm for solving the second set of equations in two-dimensional (2-D) moving inhomogeneous media is developed. Issues related to the finite-difference approximation of the spatial and temporal derivatives are discussed. FDTD solutions are obtained for a homogenous uniformly moving medium and for a stratified moving atmosphere. The first of these solutions is compared with an analytical formula for the sound pressure due to a point monochromatic source in a uniformly moving medium. The second solution is compared with predictions from before FFP.

Although the explicit emphasis of the discussion in this paper is on sound propagation in a moving inhomogeneous atmosphere, most of the derived equations are also valid for a general case of sound propagation in a moving inhomogeneous medium with an arbitrary equation of state, e.g., in the ocean with currents. Equations presented in the paper are also compared with those known in aeroacoustics.

The paper is organized as follows. In Sec. II, we consider the complete set of equations of fluid dynamics and their linearization. In Sec. III, the linearized equations are reduced to the set of three coupled equations for the sound pressure, acoustic velocity, and acoustic density. In Sec. IV, we consider the set of two coupled equations for the acoustic pressure and acoustic velocity. Numerical implementation of this set is considered in Sec. V.

II. EQUATIONS OF FLUID DYNAMICS AND THEIR LINEARIZATION

Let $\tilde{P}(\mathbf{R},t)$ be the pressure, $\tilde{\varrho}(\mathbf{R},t)$ the density, $\tilde{\mathbf{v}}(\mathbf{R},t)$ the velocity vector, and $\tilde{S}(\mathbf{R},t)$ the entropy in a medium. Here, $\mathbf{R}=(x,y,z)$ are the Cartesian coordinates, and t is time. These functions satisfy a complete set of fluid dynamic equations (e.g. Ref. 16):

$$\left(\frac{\partial}{\partial t}+\tilde{\mathbf{v}}\cdot\boldsymbol{\nabla}\right)\tilde{\mathbf{v}}+\frac{\boldsymbol{\nabla}\tilde{P}}{\tilde{\varrho}}-\mathbf{g}=\mathbf{F}/\tilde{\varrho}, \tag{1}$$

$$\left(\frac{\partial}{\partial t}+\tilde{\mathbf{v}}\cdot\boldsymbol{\nabla}\right)\tilde{\varrho}+\tilde{\varrho}\boldsymbol{\nabla}\cdot\tilde{\mathbf{v}}=\tilde{\varrho}Q, \tag{2}$$

$$\left(\frac{\partial}{\partial t}+\tilde{\mathbf{v}}\cdot\boldsymbol{\nabla}\right)\tilde{S}=0, \tag{3}$$

$$\tilde{P}=\tilde{P}(\tilde{\varrho},\tilde{S}). \tag{4}$$

In Eqs. (1)–(4), $\boldsymbol{\nabla}=(\partial/\partial x,\partial/\partial y,\partial/\partial z)$, $\mathbf{g}=(0,0,g)$ is the acceleration due to gravity, and $\mathbf{F}$ and Q characterize a force acting on the medium and a mass source, respectively. For simplicity, we do not consider the case when a passive component is dissolved in a medium (e.g., water vapor in the dry air, or salt in water). This case is considered in detail elsewhere.[9,17]

If a sound wave propagates in a medium, in Eqs. (1)–(4) $\tilde{P}$, $\tilde{\varrho}$, $\tilde{\mathbf{v}}$, and $\tilde{S}$ can be expressed in the following form: $\tilde{P}=P+p$, $\tilde{\varrho}=\varrho+\eta$, $\tilde{\mathbf{v}}=\mathbf{v}+\mathbf{w}$, and $\tilde{S}=S+s$. Here, P, ϱ, $\mathbf{v}$, and S are the ambient values (i.e., the values in the absence of a sound wave) of the pressure, density, medium velocity, and entropy in a medium, and p, η, $\mathbf{w}$, and s are their fluctuations due to a propagating sound wave. In order to obtain equations for a sound wave, Eqs. (1)–(4) are linearized with respect to p, η, $\mathbf{w}$, and s. Assuming that a sound wave is generated by the mass source Q and/or the force $\mathbf{F}$ and introducing the full derivative with respect to time $d/dt=\partial/\partial t+\mathbf{v}\cdot\boldsymbol{\nabla}$, we have

$$\frac{d\mathbf{w}}{dt}+(\mathbf{w}\cdot\boldsymbol{\nabla})\mathbf{v}+\frac{\boldsymbol{\nabla}p}{\varrho}-\frac{\eta\boldsymbol{\nabla}P}{\varrho^2}=\mathbf{F}/\varrho, \tag{5}$$

$$\frac{d\eta}{dt}+(\mathbf{w}\cdot\boldsymbol{\nabla})\varrho+\varrho\boldsymbol{\nabla}\cdot\mathbf{w}+\eta\boldsymbol{\nabla}\cdot\mathbf{v}=\varrho Q, \tag{6}$$

$$\frac{ds}{dt}+(\mathbf{w}\cdot\boldsymbol{\nabla})S=0, \tag{7}$$

$$p=\eta c^2+hs. \tag{8}$$

Here, $c=\sqrt{\partial P(\varrho,S)/\partial\varrho}$ is the adiabatic sound speed, and the parameter h is given by $h=\partial P(\varrho,S)/\partial S$. The set of Eqs. (5)–(8) provides a most general description of sound propagation in a moving inhomogeneous medium with only one component. In order to calculate p, η, $\mathbf{w}$, and s, one needs to know the ambient quantities c, ϱ, $\mathbf{v}$, P, S, and h. Note that Eqs. (5)–(8) describe the propagation of both acoustic and internal gravity waves, as well as vorticity and entropy waves (e.g., Ref. 18).

Equations (5)–(8) were derived for the first time by Blokhintzev in 1946.[17] Since then, these equations have been widely used in studies of sound propagation (e.g., Refs. 9–11). In the general case of a moving inhomogeneous medium, Eqs. (5)–(8) cannot be exactly reduced to a single equation for the sound pressure p. In the literature, Eqs. (5)–(8) have been reduced to equations for p, making use of different approximations or assumptions about the ambient medium. These equations for p were subsequently used for analytical and numerical studies of sound propagation. They are discussed in Sec. IV. Note that the equations for p known in the literature contain the following ambient quantities: c, ϱ, and $\mathbf{v}$. On the other hand, the linearized equations of fluid dynamics, Eqs. (5)–(8), contain not only c, ϱ, and $\mathbf{v}$, but

also P, S, and h. This fact indicates that the effect of P, S, and h on sound propagation is probably small for most of problems considered so far in the literature.

The effect of medium motion on sound propagation is also studied in aeroacoustics, e.g., see Refs. 12, 19–24 and references therein. In aeroacoustics, the starting equations coincide with Eqs. (1)–(4) but might also include terms describing viscosity and thermal conductivity in a medium. Using these equations of fluid dynamics, equations for sound waves are derived which have some similarities with Eqs. (5)–(8). For example, Eqs. (5)–(8) are equivalent to Eqs. (1.11) from Ref. 12, and Eq. (6) can be found in Refs. 19, 22, 23. The main difference between Eqs. (5)–(8) and those in aeroacoustics are sound sources. In atmospheric acoustics, in Eqs. (5)–(8) the sources $\mathbf{F}$ and Q are assumed to be known and are loudspeakers, car engines, etc. In aeroacoustics, these sources have to be calculated and are those due to ambient flow. Furthermore in some formulations in aeroacoustics, the left-hand side of Eq. (5) contains nonlinear terms.[21–23] Note that FDTD calculations are nowadays widely used in aeroacoustics, e.g., Refs. 19, 20, 24.

Also note that in aeroacoustics it is sometimes assumed that the ambient medium is incompressible and/or isentropic, i.e., $S=\text{const}$. Generally, these assumptions are inappropriate for atmospheric acoustics. Indeed, sound waves can be significantly scattered by density fluctuations, e.g., see Sec. 6.1.4 from Ref. 9. Furthermore, in a stratified atmosphere S depends on the height above the ground. The range of applicability of the assumption $S=\text{const}$ (which is equivalent to $s=0$ or $p=c^2\eta$) is studied in Sec. 2.2.4 from Ref. 9. For a stratified medium, this assumption is not applicable if the scale of the ambient density variations is smaller than the sound wave length or if the ambient density noticeably changes with height.

III. SET OF THREE COUPLED EQUATIONS

A. Moving medium with an arbitrary equation of state

Applying the operator $(\partial/\partial t+\tilde{\mathbf{v}}\cdot\boldsymbol{\nabla})$ to both sides of Eq. (4) and using Eq. (3), we have

$$\left(\frac{\partial}{\partial t}+\tilde{\mathbf{v}}\cdot\boldsymbol{\nabla}\right)\tilde{P}=\tilde{c}^2\left(\frac{\partial}{\partial t}+\tilde{\mathbf{v}}\cdot\boldsymbol{\nabla}\right)\tilde{\varrho}, \tag{9}$$

where $\tilde{c}^2=\partial\tilde{P}(\tilde{\varrho},\tilde{S})/\partial\tilde{\varrho}$ differs from the square of the adiabatic sound speed $c^2=\partial P(\varrho,S)/\partial\varrho$. Using Eq. (2), Eq. (9) can be written as

$$\left(\frac{\partial}{\partial t}+\tilde{\mathbf{v}}\cdot\boldsymbol{\nabla}\right)\tilde{P}+\tilde{c}^2\tilde{\varrho}\boldsymbol{\nabla}\cdot\tilde{\mathbf{v}}=\tilde{c}^2\tilde{\varrho}Q. \tag{10}$$

The next step is to linearize Eq. (10) to obtain an equation for acoustic quantities. To do so we need to calculate the value of $\tilde{c}^2=\partial\tilde{P}(\tilde{\varrho},\tilde{S})/\partial\tilde{\varrho}$ to the first order in acoustic perturbations. In this formula, we express $\tilde{\varrho}$ and $\tilde{S}$ as the sums $\tilde{\varrho}=\varrho+\eta$ and $\tilde{S}=S+s$, decompose the function P into Taylor series, and keep the terms of the first order in η and s:

$$\begin{aligned}\tilde{c}^2&=\frac{\partial\tilde{P}(\tilde{\varrho},\tilde{S})}{\partial\tilde{\varrho}}=\frac{\partial}{\partial\varrho}P(\varrho+\eta,S+s)\\&=\frac{\partial}{\partial\varrho}\left[P(\varrho,S)+\frac{\partial P(\varrho,S)}{\partial\varrho}\eta+\frac{\partial P(\varrho,S)}{\partial S}s\right]\\&=\frac{\partial P(\varrho,S)}{\partial\varrho}+\frac{\partial^2P(\varrho,S)}{\partial\varrho^2}\eta+\frac{\partial^2P(\varrho,S)}{\partial\varrho\,\partial S}s.\end{aligned} \tag{11}$$

The first term in the last line of this equation is equal to c^2. Denoting $\beta=\partial^2P(\varrho,S)/\partial\varrho^2$ and $\alpha=\partial^2P(\varrho,S)/\partial\varrho\,\partial S$, we have $\tilde{c}^2=c^2+\beta\eta+\alpha s=c^2+(c^2)'$. Here, $(c^2)'=\beta\eta+\alpha s$ are fluctuations in the squared sound speed due to a propagating sound wave. In this formula, s can be replaced by its value from Eq. (8): $s=(p-c^2\eta)/h$. As a result, we obtain the desired formula for fluctuations in the squared sound speed: $(c^2)'=(\beta-\alpha c^2/h)\eta+\alpha p/h$.

Now we can linearize Eq. (10). In this equation, we express $\tilde{P}$, $\tilde{\varrho}$, $\tilde{\mathbf{v}}$, and $\tilde{c}^2$ as the sums: $\tilde{P}=P+p$, $\tilde{\varrho}=\varrho+\eta$, $\tilde{\mathbf{v}}=\mathbf{v}+\mathbf{w}$, and $\tilde{c}^2=c^2+(c^2)'$. Linearizing the resulting equation with respect to acoustic quantities, we have

$$\frac{dp}{dt}+\varrho c^2\boldsymbol{\nabla}\cdot\mathbf{w}+\mathbf{w}\cdot\boldsymbol{\nabla}P+(c^2\eta+\varrho(c^2)')\boldsymbol{\nabla}\cdot\mathbf{v}=\varrho c^2Q. \tag{12}$$

In this equation, $(c^2)'$ is replaced by its value obtained above. As a result, we arrive at the following equation for dp/dt:

$$\begin{aligned}\frac{dp}{dt}+\varrho c^2\boldsymbol{\nabla}\cdot\mathbf{w}+\mathbf{w}\cdot\boldsymbol{\nabla}P+\{[\varrho\beta+c^2(1-\alpha\varrho/h)]\eta\\+(\alpha\varrho/h)p\}\boldsymbol{\nabla}\cdot\mathbf{v}=\varrho c^2Q.\end{aligned} \tag{13}$$

Equations (5), (6), and (13) comprise a desired set of three coupled equations for p, $\mathbf{w}$, and η. This set was obtained from linearized equations of fluid dynamics, Eqs. (5)–(8), without any approximations. The set can be used as starting equations for FDTD simulations. In this set, one needs to know the following ambient quantities: c, ϱ, $\mathbf{v}$, P, α, β, and h.

B. Set of three equations for an ideal gas

In most applications, the atmosphere can be considered as an ideal gas. In this case, the equation of state reads (e.g., Refs. 9, 17) as

$$P=P_0(\varrho/\varrho_0)^\gamma\exp[(\gamma-1)(S-S_0)/R_a], \tag{14}$$

where $\gamma=1.4$ is the ratio of specific heats at constant pressure and constant volume, R_a is the gas constant for the air, and the subscript 0 indicates reference values of P, ϱ, and S. Using Eq. (14), the sound speed c and the coefficients α, β, and h appearing in Eq. (13) can be calculated: $c^2=\gamma P/\varrho$, $\alpha=\gamma(\gamma-1)P/(\varrho R_a)$, $\beta=\gamma(\gamma-1)P/\varrho^2$, and $h=(\gamma-1)P/R_a$. Substituting these values into Eq. (13), we have

$$\frac{dp}{dt}+\varrho c^2\boldsymbol{\nabla}\cdot\mathbf{w}+\mathbf{w}\cdot\boldsymbol{\nabla}P+\gamma p\boldsymbol{\nabla}\cdot\mathbf{v}=\varrho c^2Q. \tag{15}$$

A set of Eqs. (5), (6), and (15) is a closed set of three coupled equations for p, $\mathbf{w}$, and η for the case of an ideal

gas. To solve these equations, one needs to know the following ambient quantities: c, ϱ, $\mathbf{v}$, and P.

Let us compare Eqs. (5), (6), and (15) with a closed set of equations for p and $\mathbf{w}$ from Ref. 1; see Eqs. (12) and (13) from that reference. The latter set was used in Refs. 1, 2 as starting equations for FDTD simulations of outdoor sound propagation. If $Q=0$, Eq. (15) in the present paper is essentially the same as Eq. (13) from Ref. 1. [Note that Eq. (15) is also used in aeroacoustics, e.g., Ref. 19.] Furthermore for the case of a nonabsorbing medium, Eq. (12) from Ref. 1 is given by

$$\frac{d\mathbf{w}}{dt}+(\mathbf{w}\cdot\nabla)\mathbf{v}+\frac{\nabla p}{\varrho}-\frac{p\nabla P}{\gamma P\varrho}=0. \tag{16}$$

Let us show that this equation is an approximate version of Eq. (5) in the present paper. Indeed, in Eq. (5) we replace η by its value from Eq. (8): $\eta=(p-hs)/c^2$, and assume that $s=0$. If $\mathbf{F}=0$, the resulting equation coincides with Eq. (16). Thus, for an ideal gas and $\mathbf{F}=0$ and $Q=0$, Eqs. (12) and (13) from Ref. 1 are equivalent to Eqs. (5) and (15) in the present paper if s can be set to 0. The range of applicability of the approximation $s=0$ is considered above.

IV. SET OF TWO COUPLED EQUATIONS

A. Set of equations for *p* and w

In atmospheric acoustics, Eqs. (5) and (13) can be simplified since v is always much less than c. First, using Ref. 16, it can be shown that $\nabla\cdot\mathbf{v}\sim v^3/(c^2L)$, where L is the length scale of variations in the density ϱ. Therefore, in Eq. (13) the term proportional to $\nabla\cdot\mathbf{v}$ can be ignored to order v^2/c^2. Second, in Eqs. (5) and (13) the terms proportional to ∇P can also be ignored. Indeed, in a moving inhomogeneous atmosphere ∇P is of the order v^2/c^2 so that these terms can be ignored to order v/c. Furthermore, in a stratified atmosphere, $\nabla P=-g\varrho$, where g is the acceleration due to gravity. It is known that, in linearized equations of fluid dynamics, terms proportional to g are important for internal gravity waves and can be omitted for acoustic waves.

With these approximations, Eqs. (13) and (5) become

$$\left(\frac{\partial}{\partial t}+\mathbf{v}\cdot\nabla\right)p+\varrho c^2\nabla\cdot\mathbf{w}=\varrho c^2Q, \tag{17}$$

$$\left(\frac{\partial}{\partial t}+\mathbf{v}\cdot\nabla\right)\mathbf{w}+(\mathbf{w}\cdot\nabla)\mathbf{v}+\frac{\nabla p}{\varrho}=\mathbf{F}/\varrho. \tag{18}$$

Equations (17) and (18) comprise the desired closed set of two coupled equations for p and $\mathbf{w}$. This set can also be used in FDTD simulations of sound propagation in the atmosphere. In order to solve this set, one needs to know the following ambient quantities: c, ϱ, and $\mathbf{v}$. These ambient quantities appear in equations for the sound pressure p that have been most often used for analytical and numerical studies of sound propagation in moving media. The set of Eqs. (17) and (18) is simpler than the set of three coupled equations, Eqs. (5), (6), and (13), and does not contain the ambient quantities P, α, β, and h. It can be shown that Eqs. (17) and (18) describe the propagation of acoustic and vorticity waves but do not describe entropy or internal gravity waves.

Equations (17) and (18) were derived in Ref. 25 [see also Eqs. (2.68) and (2.69) from Ref. 9] using a different approach. In these references, Eqs. (17) and (18) were derived for the case of a moving inhomogeneous medium with more than one component (e.g., humid air or salt water). Equations (17) and (18) are somewhat similar to the starting equations in FDTD simulations used in Ref. 3; see Eqs. (10) and (12) from that reference. The last of these equations coincides with Eq. (17) while the first is given by

$$\frac{\partial\mathbf{w}}{\partial t}-\mathbf{w}\times(\nabla\times\mathbf{v})+\frac{\nabla p}{\varrho_0}+\nabla[\mathbf{w}\cdot\mathbf{v}]=0. \tag{19}$$

Using vector algebra, the left-hand side of this equation can be written as a left-hand side of Eq. (18) plus an extra term $\mathbf{v}\times(\nabla\times\mathbf{w})$. Equations (10) and (12) from Ref. 3 were obtained using several assumptions that were not employed in the present paper when deriving Eqs. (17) and (18): $\partial\mathbf{v}/\partial t=\partial\varrho/\partial t=\nabla\varrho=0$, c is constant, and $\partial\mathbf{w}/\partial t\gg\mathbf{v}\times(\nabla\times\mathbf{w})$. It follows from the last inequality that the ''extra'' term $\mathbf{v}\times(\nabla\times\mathbf{w})$ in Eq. (19) can actually be omitted. Note that in Ref. 4 different starting equations were used in simulations of sound propagation in a muffler with a low Mach number flow. The use of Eq. (19) resulted in increase of stability in such simulations.

Also note that equations for p and $\mathbf{w}$ similar to Eqs. (17) and (18) are used in aeroacoustics, e.g. Refs. 20, 24. The left-hand sides of Eqs. (7) in Ref. 20 contain several extra terms in comparison with the left-hand sides of Eqs. (17) and (18) which, however, vanish if $\nabla P=0$ and $\nabla\cdot\mathbf{v}=0$. The left-hand sides of Eqs. (75) and (76) in Ref. 24 also contain extra terms in comparison with the left-hand sides of Eqs. (17) and (18), e.g., terms proportional to the gradients of c and ϱ. The right-hand sides of the equations in Refs. 20, 24 describe aeroacoustic sources and differ from those in Eqs. (17) and (18).

At the beginning of this section, we provided sufficient conditions for the applicability of Eqs. (17) and (18). Actually, the range of applicability of these equations can be much wider. Note that it is quite difficult to estimate with what accuracy one can ignore certain terms in differential equations. We will study the range of applicability of Eqs. (17) and (18) by comparing them with equations for the sound pressure p presented in Secs. IV B–IV F, which have been most often used for analytical and numerical studies of sound propagation in moving media and whose ranges of applicability are well known. This will allow us to show that Eqs. (17) and (18) have the same of a wider range of applicability than these equations for p and, in many cases, describe sound propagation to any order in v/c. For simplicity, in the rest of this section, we assume that $\mathbf{F}=0$, $Q=0$, and the medium velocity is subsonic.

B. Nonmoving medium

Consider the case of a nonmoving medium when $\mathbf{v}=0$. In this case, the set of linearized equations of fluid dynamics, Eqs. (5)–(8), can be exactly (without any approximations) reduced to a single equation for sound pressure p (e.g., see Eq. (1.11) from Ref. 11):

$$\frac{\partial}{\partial t}\left(\frac{1}{\varrho c^2}\frac{\partial p}{\partial t}\right)-\boldsymbol{\nabla}\cdot\left(\frac{\boldsymbol{\nabla} p}{\varrho}\right)=0. \tag{20}$$

For the considered case of a nonmoving medium, Eqs. (17) and (18) can also be reduced to a single equation for p. This equation coincides with Eq. (20). Therefore, Eqs. (17) and (18) describe sound propagation exactly if $\mathbf{v}=0$.

C. Homogeneous uniformly moving medium

A medium is homogeneous and uniformly moving if the ambient quantities c, $\mathbf{v}$, etc. do not depend on $\mathbf{R}$ and t. For such a medium, the linearized equations of fluid dynamics, Eqs. (5)–(8) can also be exactly reduced to a single equation for p (see Sec. 2.3.6 from Ref. 9 and references therein):

$$\left(\frac{\partial}{\partial t}+\mathbf{v}\cdot\boldsymbol{\nabla}\right)^2 p-c^2\nabla^2 p=0. \tag{21}$$

For the case of a homogeneous uniformly moving medium, Eqs. (17) and (18) can be reduced to the equation for p that coincides with Eq. (21). Therefore, Eqs. (17) and (18) describe sound propagation exactly in a homogeneous uniformly moving medium. In particular, they correctly account for terms of any order in v/c.

D. Stratified moving medium

Now let us consider the case of a stratified medium when the ambient quantities c, ϱ, $\mathbf{v}$, etc. depend only on the vertical coordinate z. We will assume that the vertical component of $\mathbf{v}$ is zero: $\mathbf{v}=(\mathbf{v}_\perp,0)$, where $\mathbf{v}_\perp$ is a horizontal component of the medium velocity vector. In this subsection, we reduce Eqs. (17) and (18) to a single equation for the spectral density of the sound pressure and show that this equation coincides with the equation for the spectral density that can be derived from Eqs. (5)–(8).

For a stratified moving medium, Eq. (17) can be written as

$$\left(\frac{\partial}{\partial t}+\mathbf{v}_\perp\cdot\boldsymbol{\nabla}_\perp\right)p+\varrho c^2\left(\boldsymbol{\nabla}_\perp\cdot\mathbf{w}_\perp+\frac{\partial w_z}{\partial z}\right)=0. \tag{22}$$

Here, $\boldsymbol{\nabla}_\perp=(\partial/\partial x,\partial/\partial y)$, and $\mathbf{w}_\perp$ and w_z are the horizontal and vertical components of the vector $\mathbf{w}=(\mathbf{w}_\perp,w_z)$. Equation (18) can be written as two equations:

$$\left(\frac{\partial}{\partial t}+\mathbf{v}_\perp\cdot\boldsymbol{\nabla}_\perp\right)w_z+\frac{1}{\varrho}\frac{\partial p}{\partial z}=0, \tag{23}$$

$$\left(\frac{\partial}{\partial t}+\mathbf{v}_\perp\cdot\boldsymbol{\nabla}_\perp\right)\mathbf{w}_\perp+w_z\mathbf{v}_\perp'+\frac{\boldsymbol{\nabla}_\perp p}{\varrho}=0. \tag{24}$$

Here, $\mathbf{v}_\perp'=d\mathbf{v}_\perp/dz$. Let p, $\mathbf{w}_\perp$, and w_z be expressed as Fourier integrals:

$$p(\mathbf{r},z,t)=\int\int d\mathbf{a}\int d\omega\,\exp(i\mathbf{a}\cdot\mathbf{r}-i\omega t)\hat{p}(\mathbf{a},z,\omega), \tag{25}$$

$$w_z(\mathbf{r},z,t)=\int\int d\mathbf{a}\int d\omega\,\exp(i\mathbf{a}\cdot\mathbf{r}-i\omega t)\hat{w}_z(\mathbf{a},z,\omega), \tag{26}$$

$$\mathbf{w}_\perp(\mathbf{r},z,t)=\int\int d\mathbf{a}\int d\omega\,\exp(i\mathbf{a}\cdot\mathbf{r}-i\omega t)\hat{\mathbf{w}}_\perp(\mathbf{a},z,\omega). \tag{27}$$

Here, $\mathbf{r}=(x,y)$ are the horizontal coordinates, $\mathbf{a}$ is the horizontal component of the wave vector, ω is the frequency of a sound wave, and $\hat{p}$, $\hat{w}_z$, and $\hat{\mathbf{w}}_\perp$ are the spectral densities of p, w_z, and $\mathbf{w}_\perp$. We substitute Eqs. (25)–(27) into Eqs. (22)–(24). As a result, we obtain a set of equations for $\hat{p}$, $\hat{w}_z$, and $\hat{\mathbf{w}}_\perp$:

$$-i(\omega-\mathbf{a}\cdot\mathbf{v}_\perp)\hat{p}+i\varrho c^2\mathbf{a}\cdot\hat{\mathbf{w}}_\perp+\varrho c^2\frac{\partial\hat{w}_z}{\partial z}=0, \tag{28}$$

$$-i(\omega-\mathbf{a}\cdot\mathbf{v}_\perp)\hat{w}_z+\frac{1}{\varrho}\frac{\partial\hat{p}}{\partial z}=0, \tag{29}$$

$$-i(\omega-\mathbf{a}\cdot\mathbf{v}_\perp)\hat{\mathbf{w}}_\perp+\mathbf{v}_\perp'\hat{w}_z+\frac{i\mathbf{a}\hat{p}}{\varrho}=0. \tag{30}$$

After some algebra, this set of equations can be reduced to a single equation for $\hat{p}$:

$$\frac{\partial^2\hat{p}}{\partial z^2}+\left(\frac{2\mathbf{a}\cdot\mathbf{v}_\perp'}{\omega-\mathbf{a}\cdot\mathbf{v}_\perp}-\frac{\varrho'}{\varrho}\right)\frac{\partial\hat{p}}{\partial z}+\left(\frac{(\omega-\mathbf{a}\cdot\mathbf{v}_\perp)^2}{c^2}-a^2\right)\hat{p}=0, \tag{31}$$

where $\varrho'=d\varrho/dz$.

For the considered case of a stratified moving medium, a single equation for $\hat{p}$ can also be derived from Eqs. (5)–(8) without any approximations. This equation for p is given by Eq. (2.61) from Ref. 9. Setting $g=0$ in this equation (i.e. ignoring internal gravity waves) one obtains Eq. (31). Therefore, Eqs. (17) and (18) describe sound propagation exactly in a stratified moving medium, and, hence, correctly account for terms of any order in v/c.

E. Turbulent medium

Probably the most general of the equations describing the propagation of a monochromatic sound wave in turbulent media with temperature and velocity fluctuations is given by Eq. (6.1) from Ref. 9:

$$\left[\Delta+k_0^2(1+\varepsilon)-\left(\boldsymbol{\nabla}\ln\frac{\varrho}{\varrho_0}\right)\cdot\boldsymbol{\nabla}-\frac{2i}{\omega}\frac{\partial v_i}{\partial x_j}\frac{\partial^2}{\partial x_i\partial x_j}+\frac{2ik_0}{c_0}\mathbf{v}\cdot\boldsymbol{\nabla}\right]p(\mathbf{R})=0. \tag{32}$$

Here, $\Delta=\partial^2/\partial x^2+\partial^2/\partial y^2+\partial^2/\partial z^2$; $\varepsilon=c_0^2/c^2-1$; k_0, c_0, and ϱ_0 are the reference values of the wave number, adiabatic sound speed, and density; x_1, x_2, x_3 stand for x, y, z; $v_1=v_x$, $v_2=v_y$, $v_3=v_z$ are the components of the medium velocity vector $\mathbf{v}$; and repeated subscripts are summed from 1 to 3. Furthermore, the dependence of the sound pressure on the time factor $\exp(-i\omega t)$ is omitted.

The range of applicability of Eq. (32) is considered in detail in Sec. 2.3 from Ref. 9. This equation was used for calculations of the sound scattering cross section per unit volume of a sound wave propagating in a turbulent medium with temperature and velocity fluctuations. Also it was employed as a starting equation for developing a theory of mul-

tiple scattering of a sound wave propagating in such a turbulent medium; see Ref. 9 and references therein. Furthermore, starting from Eq. (32), parabolic and wide-angle parabolic equations were derived and used in analytical and numerical studies of sound propagation in a turbulent medium, e.g., Ref. 26. For example, a parabolic equation deduced from Eq. (32) reads as

$$2ik_0\frac{\partial p}{\partial x}+\Delta_\perp p+2k_0^2\left(1+\frac{\varepsilon_{\mathrm{mov}}}{2}\right)p=0. \tag{33}$$

Here, the predominant direction of sound propagation coincides with the x-axis, $\Delta_\perp=(\partial^2/\partial y^2,\partial^2/\partial z^2)$, and $\varepsilon_{\mathrm{mov}}=\varepsilon-2v_x/c_0$.

In Ref. 9, Eq. (32) was derived starting from the set of Eqs. (17) and (18) and using some approximations. Therefore, this set has the same or a wider range of applicability than equations for p that have been used in the literature for analytical and numerical studies of sound propagation in a turbulent medium with temperature and velocity fluctuations.

F. Geometrical acoustics

Sound propagation in a moving inhomogeneous medium is often described in geometrical acoustics approximation which is applicable if the sound wavelength is much smaller than the scale of medium inhomogeneities. In geometrical acoustics, the phase of a sound wave can be obtained as a solution of the eikonal equation, and its amplitude from the transport equation. In this subsection, starting from Eqs. (17) and (18), we derive eikonal and transport equations and show that they are in agreement with those deduced from Eqs. (5)–(8).

Let us express p and $\mathbf{w}$ in the following form:

$$p(\mathbf{R},t)=\exp(ik_0\Theta(\mathbf{R},t))p_A(\mathbf{R},t), \tag{34}$$

$$\mathbf{w}(\mathbf{R},t)=\exp(ik_0\Theta(\mathbf{R},t))\mathbf{w}_A(\mathbf{R},t). \tag{35}$$

Here, $\Theta(\mathbf{R},t)$ is the phase function, and p_A and $\mathbf{w}_A$ are the amplitudes of p and $\mathbf{w}$. Substituting Eqs. (34) and (35) into Eqs. (17) and (18), we have

$$ik_0\left(\varrho c^2\mathbf{w}_A\cdot\boldsymbol{\nabla}\Theta+p_A\frac{d\Theta}{dt}\right)=-\frac{dp_A}{dt}-\varrho c^2\boldsymbol{\nabla}\cdot\mathbf{w}_A, \tag{36}$$

$$ik_0\left(\mathbf{w}_A\frac{d\Theta}{dt}+\frac{p_A\boldsymbol{\nabla}\Theta}{\varrho}\right)=-\frac{d\mathbf{w}_A}{dt}-(\mathbf{w}_A\cdot\boldsymbol{\nabla})\mathbf{v}-\frac{\boldsymbol{\nabla}p_A}{\varrho}. \tag{37}$$

In geometrical acoustics, p_A and $\mathbf{w}_A$ are expressed as a series in a small parameter proportional to $1/k_0$:

$$p_A=p_1+\frac{p_2}{ik_0}+\frac{p_3}{(ik_0)^2}+\ldots, \tag{38}$$

$$\mathbf{w}_A=\mathbf{w}_1+\frac{\mathbf{w}_2}{ik_0}+\frac{\mathbf{w}_3}{(ik_0)^2}+\ldots. \tag{39}$$

Substituting Eqs. (38) and (39) into Eqs. (36) and (37) and equating terms proportional to k_0, we arrive at a set of equations:

$$\varrho c^2\mathbf{w}_1\cdot\boldsymbol{\nabla}\Theta+p_1\frac{d\Theta}{dt}=0, \tag{40}$$

$$\mathbf{w}_1\frac{d\Theta}{dt}+p_1\frac{\boldsymbol{\nabla}\Theta}{\varrho}=0. \tag{41}$$

Equating terms proportional to k_0^0, we obtain another set:

$$\varrho c^2\mathbf{w}_2\cdot\boldsymbol{\nabla}\Theta+p_2\frac{d\Theta}{dt}=-\frac{dp_1}{dt}-\varrho c^2\boldsymbol{\nabla}\cdot\mathbf{w}_1, \tag{42}$$

$$\mathbf{w}_2\frac{d\Theta}{dt}+\frac{p_2\boldsymbol{\nabla}\Theta}{\varrho}=-\frac{d\mathbf{w}_1}{dt}-(\mathbf{w}_1\cdot\boldsymbol{\nabla})\mathbf{v}-\frac{\boldsymbol{\nabla}p_1}{\varrho}. \tag{43}$$

From Eq. (41), we have

$$\mathbf{w}_1=-\frac{p_1}{\varrho}\frac{\boldsymbol{\nabla}\Theta}{d\Theta/dt}. \tag{44}$$

Substituting this value of $\mathbf{w}_1$ into Eq. (40), we obtain

$$\left[\left(\frac{d\Theta}{dt}\right)^2-c^2(\boldsymbol{\nabla}\Theta)^2\right]p_1=0. \tag{45}$$

From this equation, we obtain an eikonal equation for the phase function:

$$\frac{d\Theta}{dt}=-c|\boldsymbol{\nabla}\Theta|. \tag{46}$$

Here, a sign in front of $|\boldsymbol{\nabla}\Theta|$ is chosen in accordance with the time convention $\exp(-i\omega t)$. Equation (46) coincides exactly with the eikonal equation for sound waves in a moving inhomogeneous medium (e.g., see Eq. (3.15) from Ref. 9) which can be derived from Eqs. (5)–(8) in a geometrical acoustics approximation. Thus, in this approximation, Eqs. (17) and (18) exactly describe the phase of a sound wave and, hence, account for terms of any order in v/c.

Substituting the value of $d\Theta/dt$ from Eq. (46) into Eq. (44), we have

$$\mathbf{w}_1=\frac{p_1}{\varrho}\frac{\boldsymbol{\nabla}\Theta}{c|\boldsymbol{\nabla}\Theta|}=\frac{p_1\mathbf{n}}{\varrho c}, \tag{47}$$

where $\mathbf{n}=\boldsymbol{\nabla}\Theta/|\boldsymbol{\nabla}\Theta|$ is the unit vector normal to the phase front. Now we multiply Eq. (42) by $d\Theta/dt$ and multiply Eq. (43) by $c^2\varrho\boldsymbol{\nabla}\Theta$. Then, we subtract the latter equation from the former. After some algebra and using Eq. (46), it can be shown that the sum of all terms proportional to p_2 and $\mathbf{w}_2$ is zero. The resulting equation reads as

$$\frac{dp_1}{dt}+c\mathbf{n}\cdot\boldsymbol{\nabla}p_1+\varrho c\mathbf{n}\cdot\frac{d\mathbf{w}_1}{dt}+\varrho c\mathbf{n}\cdot(\mathbf{w}_1\cdot\boldsymbol{\nabla})\mathbf{v}+\varrho c^2\boldsymbol{\nabla}\cdot\mathbf{w}_1=0. \tag{48}$$

In this equation, $\mathbf{w}_1$ is replaced by its value given by Eq. (47). As a result, we obtain

$$\frac{\varrho\mathbf{n}}{c}\cdot\frac{d}{dt}\left(\frac{\mathbf{n}p_1}{\varrho c}\right)+\frac{1}{c^2}\frac{dp_1}{dt}+\frac{\mathbf{n}\cdot\boldsymbol{\nabla}p_1}{c}+\varrho\boldsymbol{\nabla}\cdot\left(\frac{\mathbf{n}p_1}{\varrho c}\right)+\frac{p_1\mathbf{n}\cdot(\mathbf{n}\cdot\boldsymbol{\nabla})\mathbf{v}}{c^2}=0. \tag{49}$$

In geometrical acoustics, the amplitude p_A of the sound pressure is approximated by p_1. Equation (49) is a closed equation for p_1; i.e., it is a transport equation.

The second term on the left-hand side of Eq. (49) can be written as

$$\frac{1}{c^2}\frac{dp_1}{dt}=\frac{d}{dt}\left(\frac{p_1}{c^2}\right)+\frac{p_1}{c^4}\frac{dc^2}{dt}=\frac{d}{dt}\left(\frac{p_1}{c^2}\right)+\frac{p_1}{c^4}\frac{\beta d\varrho}{dt}. \quad (50)$$

Here, we used the formula $dc^2/dt=\beta d\varrho/dt$; see Eq. (2.63) from Ref. 9. According to Eq. (2), $d\varrho/dt$ in Eq. (50) can be replaced with $-\varrho\nabla\cdot\mathbf{v}$. When deriving Eqs. (17) and (18), terms proportional to $\nabla\cdot\mathbf{v}$ were ignored. Therefore, the last term on the right-hand side of Eq. (50) should also be ignored. In this case, Eq. (49) can be written as

$$\frac{\varrho\mathbf{n}}{c}\cdot\frac{d}{dt}\left(\frac{\mathbf{n}p_1}{\varrho c}\right)+\frac{d}{dt}\left(\frac{p_1}{c^2}\right)+\frac{\mathbf{n}\cdot\nabla p_1}{c}+\varrho\nabla\cdot\left(\frac{\mathbf{n}p_1}{\varrho c}\right)+\frac{p_1\mathbf{n}\cdot(\mathbf{n}\cdot\nabla)\mathbf{v}}{c^2}=0. \quad (51)$$

This equation coincides with Eq. (3.18) from Ref. 9 if in the latter equation terms proportional to $\nabla\cdot\mathbf{v}$ are ignored. Equation (3.18) is an exact transport equation for p_1 in the geometrical acoustics derived from Eqs. (5)–(8). Thus, if the terms proportional to $\nabla\cdot\mathbf{v}$ are ignored, Eqs. (17) and (18) exactly describe the amplitude of a sound wave in a geometrical acoustics approximation, and correctly account for terms of any order in v/c. Note that in Ref. 9 starting from the transport equation, Eq. (3.18), a law of acoustic energy conservation in geometrical acoustics of moving media is derived; see Eq. (3.21) from that reference. Since Eq. (51) coincides with Eq. (3.18), the same law [i.e., Eq. (3.21) from Ref. 9] can be derived from Eq. (51) provided that the terms proportional to $\nabla\cdot\mathbf{v}$ are ignored.

G. Discussion

Thus, by comparing a set of Eqs. (17) and (18) with the equations for p which are widely used in atmospheric acoustics, we determined that this set has the same or a wider range of applicability than these equations for p. Note that there are other equations for p known in the literature (see Refs. 9, 11, 17 and references therein): Monin's equation, Pierce's equations, equation for the velocity quasi-potential, the Andreev–Rusakov–Blokhintzev equation, etc. Most of these equations have narrower ranges of applicability than the equations presented above and have been seldom used for calculations of p.

V. NUMERICAL IMPLEMENTATION

In this section, we describe simple algorithms for FDTD solutions of Eqs. (17) and (18) in the two spatial dimensions x and y. Isolating the partial derivatives with respect to time on the left side of these equations, we have

$$\frac{\partial p}{\partial t}=-\left(v_x\frac{\partial}{\partial x}+v_y\frac{\partial}{\partial y}\right)p-\kappa\left(\frac{\partial w_x}{\partial x}+\frac{\partial w_y}{\partial y}\right)+\kappa Q, \quad (52)$$

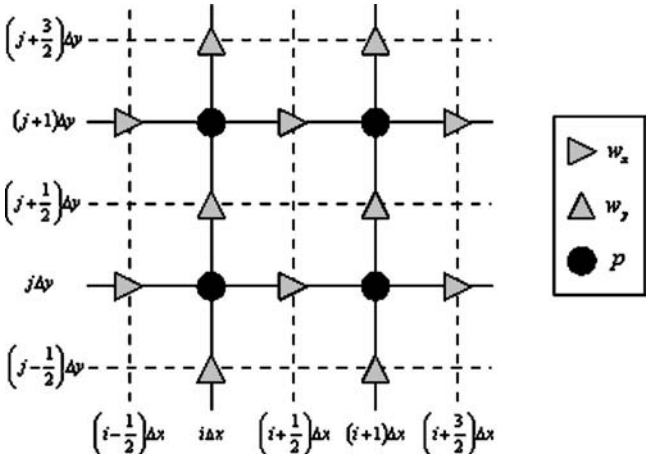

FIG. 1. Spatially staggered finite-difference grid used for the calculations in this article.

$$\frac{\partial w_x}{\partial t}=-\left(w_x\frac{\partial}{\partial x}+w_y\frac{\partial}{\partial y}\right)v_x-\left(v_x\frac{\partial}{\partial x}+v_y\frac{\partial}{\partial y}\right)w_x-b\frac{\partial p}{\partial x}+bF_x, \quad (53)$$

$$\frac{\partial w_y}{\partial t}=-\left(w_x\frac{\partial}{\partial x}+w_y\frac{\partial}{\partial y}\right)v_y-\left(v_x\frac{\partial}{\partial x}+v_y\frac{\partial}{\partial y}\right)w_y-b\frac{\partial p}{\partial y}+bF_y, \quad (54)$$

where $b=1/\rho$ is the mass buoyancy and $\kappa=\rho c^2$ is the adiabatic bulk modulus. In Eqs. (52)–(54), the subscripts x and y indicate components along the corresponding coordinate axes.

The primary numerical issues pertinent to solving these equations in a moving inhomogeneous medium are summarized and addressed in Secs. V A–V C. Example calculations are provided in Secs. V D and V E.

A. Spatial finite-difference approximations

The spatial finite-difference (FD) network considered here stores the pressure and particle velocities on a grid that is staggered in space, as shown in Fig. 1. The pressure is stored at integer node positions, namely $x=i\,\Delta x$ and $y=j\,\Delta y$, where i and j are integers and Δx and Δy are the grid intervals in the x- and y-directions. The x-components of the acoustic velocity, w_x, are staggered (offset) by $\Delta x/2$ in the x-direction. The y-components of the acoustic velocity, w_y, are staggered by $\Delta y/2$ in the y-direction. This staggered grid design is widely used for wave propagation calculations in nonmoving media.[27–30] Here we furthermore store v_x and F_x at the w_x nodes, and v_y and F_y at the w_y nodes. The quantities b, κ, and Q are stored at the pressure nodes.

For simplicity, we consider in this article only a second-order accurate, spatially centered FD scheme. A centered solution of Eqs. (52)–(54) requires an evaluation of each of the terms of the right-hand sides of these equations at the grid nodes where the field variable on the left-hand side is stored. One of the main motivations for using the spatially staggered

grid is that it conveniently provides compact, centered spatial differences for many of the derivatives in Eqs. (52)–(54). For example, $\partial w_x/\partial x$ in Eq. (52) is

$$\partial w_x(i\,\Delta x, j\,\Delta y, t)/\partial x \simeq \{w_x[(i+1/2)\Delta x, j\,\Delta y, t] - w_x[(i-1/2)\Delta x, j\,\Delta y, t]\}/\Delta x \quad (55)$$

and $\partial p/\partial y$ in Eq. (54) is

$$\partial p[i\,\Delta x,(j+1/2)\Delta y,t]/\partial y \simeq \{p[i\,\Delta x,(j+1)\Delta y,t]-p[i\,\Delta x,j\,\Delta y,t]\}/\Delta y. \quad (56)$$

The derivatives $\partial p/\partial x$ and $\partial w_y/\partial y$ follow similarly. The body source terms can all be evaluated directly, since they are already stored at the grid nodes where the FD approximations are centered. The same is true of κ, which is stored at the pressure grid nodes and needed in Eq. (52). Regarding Eqs. (53) and (54), the values for b can be determined at the needed locations by averaging neighboring grid points.

The implementation of the remaining terms, particular to the moving medium, is somewhat more complicated. For example, the derivatives of the pressure field in Eq. (52), $\partial p/\partial x$ and $\partial p/\partial y$, cannot be centered at $x=i\,\Delta x$ and $y=j\,\Delta y$ from approximations across a single grid interval. Centered approximations can be formed across two grid intervals, however, as suggested in Ref. 2. For example,

$$\partial p(i\,\Delta x, j\,\Delta y, t)/\partial x \simeq \{p[(i+1)\Delta x, j\,\Delta y, t]-p[(i-1)\Delta x, j\,\Delta y, t]\}/2\Delta x. \quad (57)$$

Neighboring grid points can be averaged to find the wind velocity components v_x and v_y at $x=i\,\Delta x$ and $y=j\,\Delta y$, which multiply the derivatives $\partial p/\partial x$ and $\partial p/\partial y$, respectively, in Eq. (52). Similarly, the spatial derivatives of the particle velocities in Eqs. (53) and (54) can be approximated over two grid intervals. In Eq. (53), the quantities w_y and v_y (multiplying the derivatives $\partial v_x/\partial y$ and $\partial w_x/\partial y$, respectively) are needed at the grid point $x=(i+1/2)\Delta x$ and $y=j\,\Delta y$. Referring to Fig. 1, a reasonable way to obtain these quantities would be to average the four closest grid nodes:

$$w_y[(i+1/2)\Delta x, j\,\Delta y, t] \simeq \frac{1}{4}\{w_y[(i+1)\Delta x,(j+1/2)\Delta y,t] + w_y[i\,\Delta x,(j+1/2)\Delta y,t] + w_y[(i+1)\Delta x,(j-1/2)\Delta y,t] + w_y[i\,\Delta x,(j-1/2)\Delta y,t]\}, \quad (58)$$

and likewise for v_y. The quantities w_x and v_x, multiplying the derivatives $\partial v_y/\partial x$ and $\partial w_y/\partial x$ in Eq. (54), can be obtained similarly.

B. Advancing the solution in time

Let us define the functions f_p, f_x, and f_y as the right-hand sides of Eqs. (52), (53), and (54), respectively. For example, we write

$$\frac{\partial p(i\,\Delta x, j\,\Delta y, t)}{\partial t} = f_p[i\,\Delta x, j\,\Delta y, \mathbf{p}(t), \mathbf{w}_x(t), \mathbf{w}_y(t), \mathbf{s}(t)], \quad (59)$$

where $\mathbf{p}(t)$, $\mathbf{w}_x(t)$, and $\mathbf{w}_y(t)$ are matrices containing the pressures and acoustic velocities at all available grid nodes. For convenience, $\mathbf{s}(t)$ is used here as short hand for the combined source and medium properties (b, κ, v_x, v_y, Q, F_x, and F_y) at all available grid nodes. (Note that $f_p[i\,\Delta x, j\,\Delta y, \mathbf{p}(t), \mathbf{w}_x(t), \mathbf{w}_y(t), \mathbf{s}(t)]$ in actuality depends only on the fields at a small number of neighboring grid points of $(i\,\Delta x, j\,\Delta y)$ when second-order spatial differencing is used. The notation here is general enough, though, to accommodate spatial differencing of an arbitrarily high order.)

For a nonmoving medium, the solution is typically advanced in time using a staggered temporal grid, in which the pressures are stored at the integer time steps $t=l\,\Delta t$ and the particle velocities at the half-integer time steps $t=(l+1/2)\Delta t$.[27–30] The acoustic velocities and pressures are updated in an alternating "leap-frog" fashion, with the fields from the previous time step being overwritten in place. Considering the moving media equations, approximation of the time derivative in Eq. (59) with a finite difference centered on $t=(l+1/2)\Delta t$ (that is, $\partial p[i\,\Delta x, j\,\Delta y,(l+1/2)\Delta t]/\partial t \simeq \{p[i\,\Delta x, j\,\Delta y,(l+1)\Delta t]-p[i\,\Delta x, j\,\Delta y, l\,\Delta t]\}/\Delta t$) results in the following equation for updating the pressure field:

$$p[i\,\Delta x, j\,\Delta y,(l+1)\Delta t] = p[i\,\Delta x, j\,\Delta y, l\,\Delta t] + \Delta t\, f_p[i\,\Delta x, j\,\Delta y, \mathbf{p}[(l+1/2)\Delta t], \mathbf{w}_x[(l+1/2)\Delta t], \mathbf{w}_y[(l+1/2)\Delta t], \mathbf{s}[(l+1/2)\Delta t]]. \quad (60)$$

Note that this equation requires the pressure field at the half-integer time steps, i.e., $t=(l+1/2)\Delta t$. In the staggered leap-frog scheme, however, the pressure is unavailable at the half-integer time steps. A similar centered approximation for the acoustic velocities indicates that they are needed on the integer time steps in order to advance the solution, which is again problematic. If one attempts to address this problem by linearly interpolating between adjacent time steps (i.e., by setting $\mathbf{p}[(l+1/2)\Delta t] \simeq \{\mathbf{p}[l\,\Delta t]+\mathbf{p}[(l+1)\Delta t]\}/2$ in Eq. (60)), explicit updating equations (a solution of Eq. (60) for $p[i\,\Delta x, j\,\Delta y,(l+1)\Delta t]$ that does not require the pressure field at nearby grid points at the time step $t=(l+1)\Delta t$) cannot be obtained. Hence the customary staggered leap-frog approach does not lead to an explicit updating scheme for the acoustic fields in a moving medium. The staggered leap-frog scheme can be rigorously implemented only when the terms particular to the moving medium (those involving v_x and v_y) are removed from Eqs. (52)–(54).

A possible work-around would be to use the pressure field $\mathbf{p}(l\,\Delta t)$ in place of $\mathbf{p}[(l+1/2)\Delta t]$ when evaluating f_p, and $\mathbf{w}_x[(l-1/2)\Delta t]$ and $\mathbf{w}_y[(l-1/2)\Delta t]$ in place of $\mathbf{w}_x(l\,\Delta t)$ and $\mathbf{w}_y(l\,\Delta t)$ when evaluating f_x and f_y. This nonrigorous procedure uses the Euler (forward difference) method to evaluate the moving-media terms while maintaining the leap-frog approach for the remaining terms. From a programming standpoint, the algorithm proceeds in essen-

tially the same manner as the staggered leap-frog method for a nonmoving medium. The calculations in Ref. 2 appear to use such a procedure. But the stability and accuracy of this algorithm are unclear. An alternative is provided in Ref. 4, which uses a perturbative solution based on the assumption that the flow velocity is small.

Here we would like to develop a general technique that is applicable to high Mach numbers. The simplest way to accomplish this is to abandon the staggered temporal grid and form centered finite differences over *two* time steps. The pressure updating equation, based on the approximation $\partial p(i\,\Delta x,\ j\,\Delta y,\ l\,\Delta t)/\partial t \simeq \{p[i\,\Delta x,\ j\,\Delta y,(l+1)\Delta t] - p[i\ \Delta x,\ j\Delta y,(l-1)\Delta t]\}/2\,\Delta t$, is

$$\begin{aligned} p[i\,\Delta x, j\,\Delta y,(l+1)\Delta t] &= p[i\,\Delta x, j\,\Delta y,(l-1)\Delta t] \\ &\quad + 2\,\Delta t\, f_p[i\,\Delta x, j\,\Delta y, \mathbf{p}(l\,\Delta t), \mathbf{w}_x(l\,\Delta t), \\ &\qquad \mathbf{w}_y(l\,\Delta t), \mathbf{s}(l\,\Delta t)]. \end{aligned} \tag{61}$$

Similarly, we derive

$$\begin{aligned} w_x[(i+1/2)\Delta x, j\,\Delta y,(l+1)\Delta t] &= w_x[(i+1/2)\Delta x, j\,\Delta y,(l-1)\Delta t] + 2\,\Delta t\, f_x[(i \\ &\quad + 1/2)\Delta x, j\,\Delta y, \mathbf{p}(l\,\Delta t), \mathbf{w}_x(l\,\Delta t), \mathbf{w}_y(l\,\Delta t), \mathbf{s}(l\,\Delta t)], \end{aligned} \tag{62}$$

$$\begin{aligned} w_y[i\,\Delta x,(j+1/2)\Delta y,(l+1)\Delta t] &= w_y[i\,\Delta x,(j+1/2)\Delta y,(l-1)\Delta t] \\ &\quad + 2\,\Delta t\, f_y[i\,\Delta x,(j+1/2)\Delta y, \mathbf{p}(l\,\Delta t), \mathbf{w}_x \\ &\qquad (l\,\Delta t), \mathbf{w}_y(l\,\Delta t), \mathbf{s}(l\,\Delta t)]. \end{aligned} \tag{63}$$

Somewhat confusingly, this general temporal updating scheme has also been called the ''leap-frog'' scheme in the literature,[31] since it involves alternately overwriting the wavefield variables at even and odd integer time steps based on calculations with the fields at the intervening time step. We call this scheme here the *nonstaggered leap-frog*. The primary disadvantage, in comparison to the staggered leap-frog scheme, is that the fields must be stored over two time steps, rather than just one. Additionally, the numerical dispersion and instability characteristics are inferior to those of the conventional staggered scheme due to the advancement of the wavefield variables over two time steps instead of one. On the other hand, the nonstaggered leap-frog does provide a simple and rigorous centered finite-difference scheme that is not specialized to low Mach number flows. Other common numerical integration methods, such as the Runge–Kutta family, can also be readily applied to the nonstaggered-in-time grid. Some of the calculations following later in this section use a fourth-order Runge–Kutta method, which is described in Ref. 32 and many other texts. We have also developed a staggered-in-time method that is valid for high Mach numbers but requires the fields to be stored over two time levels. This method was briefly discussed in Ref. 6.

Note that our present numerical modeling efforts are directed toward demonstrating the applicability and feasibility of FDTD techniques for simulating sound propagation in a moving atmosphere. We have not undertaken a comprehensive comparative analysis of the many alternative numerical strategies available for the solution of Eqs. (17) and (18). However, several of these approaches (including the pseudospectral method, higher-order spatial and/or temporal finite-difference operators, and the dispersion relation preserving (DRP) technique) yield accurate simulations of sound propagation with fewer grid intervals per wavelength compared with our numerical examples. In particular, the DRP method, involving optimized numerical values of the finite-difference operator coefficients (e.g., Ref. 18), can be readily introduced into our FDTD algorithmic framework.

C. Dependence of grid increments on Mach number

For numerical stability of the 2-D FDTD calculation, the time step Δt and grid spacing Δr must be chosen to satisfy the Courant condition, $C<1/\sqrt{2}$ (e.g., see Ref. 33), where the Courant number is defined as

$$C=\frac{u\,\Delta t}{\Delta r}. \tag{64}$$

Here, u is the speed at which the sound energy propagates. [For a nonuniform grid, $\Delta r=1/\sqrt{(\Delta x)^{-2}+(\Delta y)^{-2}}$.] Since the grid spacing must generally be a small fraction of a wavelength for good numerical accuracy, the Courant condition in practice imposes a limitation on the maximum time step possible for stable calculations. An even smaller time step may be necessary for good accuracy, however.

Let us consider the implications of the Courant condition for propagation in a uniform flow. In this case, u is determined by a combination of the sound speed and wind velocity. In the downwind direction, we have $u=u_+=c+v$. In the upwind direction, $u=u_-=c-v$. The wavelengths in these two directions are $\lambda_+=(c+v)/f$ and $\lambda_-=(c-v)/f$, respectively, where f is the frequency. Since the wavelength is shortest in the *upwind* direction, the value of λ_- dictates the grid spacing. We set

$$\Delta r=\frac{\lambda_-}{N}=\frac{\lambda}{N}(1-M), \tag{65}$$

where N is the number of grid points per wavelength in the upwind direction, $M=v/c$ is the Mach number, and $\lambda=c/f$ is the wavelength for the medium at rest. If N is to be fixed at a constant value, a finer grid is required as M increases. Regarding the time step, the Courant condition implies

$$\Delta t<\frac{\lambda_-}{\mathrm{Nu}}. \tag{66}$$

This condition is most difficult to meet when u is largest, which is the case in the *downwind* direction. Therefore we must use u_+ in the preceding inequality if we are to have accurate results throughout the domain; specifically, we must set

$$\Delta t<\frac{\lambda_-}{\mathrm{Nu}_+}=\frac{1}{Nf}\,\frac{1-M}{1+M}. \tag{67}$$

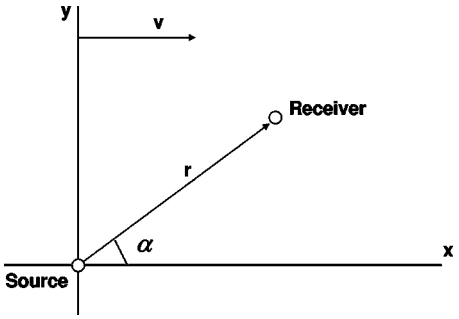

FIG. 2. The geometry of the problem.

Therefore the time step must also be shortened as M increases. For example, the time step at $M=1/3$ must be 1/2 the value necessary at $M=0$. At $M=2/3$, the time step must be 1/5 the value at $M=0$. The reduction of the required time step and grid spacing combine to make calculations at large Mach numbers computationally expensive.

D. Example calculations

In this subsection, we use the developed algorithm for FDTD solutions of Eqs. (52)–(54) to compute the sound field p in a 2-D homogeneous uniformly moving medium. The geometry of the problem is shown in Fig. 2. A point monochromatic source is located at the origin of the Cartesian coordinate system x,y. The medium velocity $\mathbf{v}$ is parallel to the x-axis. We will first obtain an analytical formula for p for this geometry.

In a homogeneous uniformly moving medium, c, ϱ, and $\mathbf{v}$ are constant so that $\boldsymbol{\nabla}\cdot\mathbf{v}=0$ and $\boldsymbol{\nabla}P=0$. Therefore, Eqs. (17) and (18) describe sound propagation exactly for this case and are valid for an arbitrary value of the Mach number M. They can be written as

$$\left(\frac{\partial}{\partial t}+\mathbf{v}\cdot\boldsymbol{\nabla}\right)p+\varrho c^2\boldsymbol{\nabla}\cdot\mathbf{w}=\varrho c^2 Q, \tag{68}$$

$$\left(\frac{\partial}{\partial t}+\mathbf{v}\cdot\boldsymbol{\nabla}\right)\mathbf{w}+\frac{\boldsymbol{\nabla}p}{\varrho}=0. \tag{69}$$

Here, p and $\mathbf{w}$ are functions of the coordinates x, y and time t, $\boldsymbol{\nabla}=(\partial/\partial x,\partial/\partial y)$, and the function Q is given by

$$Q=\frac{2iA}{\varrho\omega}e^{-i\omega t}\delta(x)\,\delta(y), \tag{70}$$

where δ is the delta function and the factor A characterizes the source amplitude. In Eqs. (68) and (69), for simplicity, it is assumed that $\mathbf{F}=0$.

Assuming that $v<c$, the following solution of Eqs. (68) and (69) is obtained in the Appendix:

$$p(r,\alpha,M)=\frac{iA}{2(1-M^2)^{3/2}}\left(H_0^{(1)}(\xi)-\frac{iM\cos\alpha}{\sqrt{1-M^2\sin^2\alpha}}H_1^{(1)}(\xi)\right)\times\exp\left[-\frac{ikMr\cos\alpha}{1-M^2}\right]. \tag{71}$$

Here, $k=\omega/c$, $H_0^{(1)}$, and $H_1^{(1)}$ are the Hankel functions, $\xi=kr\sqrt{1-M^2\sin^2\alpha}/(1-M^2)$, and r and α are the polar coordinates shown in Fig. 2. For $kr\gg1$, the Hankel functions can be approximated by their asymptotics. This results in the desired formula for the sound pressure:

$$p(r,\alpha,M)=\frac{A(\sqrt{1-M^2\sin^2\alpha}-M\cos\alpha)}{\sqrt{2\pi kr}(1-M^2)(1-M^2\sin^2\alpha)^{3/4}}\times\exp\left[\frac{i(\sqrt{1-M^2\sin^2\alpha}-M\cos\alpha)kr}{1-M^2}+\frac{i\pi}{4}\right]. \tag{72}$$

Note that a sound field due to a point monochromatic source in a 2-D homogeneous uniformly moving medium was also studied in Ref. 18 by a different approach. The phase factor obtained in that reference is essentially the same as that in Eq. (72). Only a general expression for the amplitude factor was presented in Ref. 18 which does not allow a detailed comparison with the amplitude factor in Eq. (72).

Let us now consider the FDTD calculations of the sound field for the geometry in Fig. 2. In these calculations, the source consists of a finite-duration harmonic signal with a cosine taper function applied at the beginning and the end. The tapering alleviates numerical dispersion of high frequencies, which becomes evident when there is an abrupt change in the source emission. The tapered source equation is

$$\tilde{Q}(t)=\begin{cases}(1/2)[1-\cos(\pi t/T_1)]\cos(2\pi f+\phi), & 0\leqslant t<T_1,\\ \cos(2\pi f+\phi), & T_1\leqslant t\leqslant T-T_2,\\ (1/2)[1+\cos(\pi(t-T)/T_2)]\cos(2\pi f+\phi), & T-T_2<t\leqslant T,\\ 0, \quad \text{otherwise.}\end{cases} \tag{73}$$

Here, ϕ is the source phase, T_1 is the duration of the initiation taper, and T_2 is the duration of the termination taper. All calculations in this paper use tapering over an interval of 3 periods in the harmonic wave ($T_1=T_2=3/f$) and a total signal duration of 10 periods ($T=10/f$).

Figure 3 shows the pressure field for a 100 Hz source in a uniform Mach 0.3 flow. The field is shown at 0.11 s, or 0.01 s after the source has been turned off. The distance between wave fronts is smaller upwind than downwind. The calculations use the fourth-order Runge–Kutta method with a staggered spatial grid and a nonstaggered temporal grid. The spatial domain is 100 m by 100 m, with 800 grid points in each direction. This results in approximately 19 grid points per wavelength in the upwind direction. The time step was set to 0.145 ms, which implies a Courant number of 0.40 in a nonmoving medium but 0.52 in the downwind direction of the $M=0.3$ flow. Using the run shown in Fig. 3, the azimuthal dependence of the normalized sound pressure magnitude $|p(r,\alpha,M)/p(r,0,0)|$ for values of kr ranging from 1 to 100 was compared to the theoretical far-field result calculated from Eq. (72). Excellent agreement was found between theoretical predictions and FDTD simulations for $kr\gtrsim10$.

The azimuthal dependence of $|p(r,\alpha,M)/p(r,0,0)|$ at $kr=20$ is compared for several numerical methods in Fig. 4.

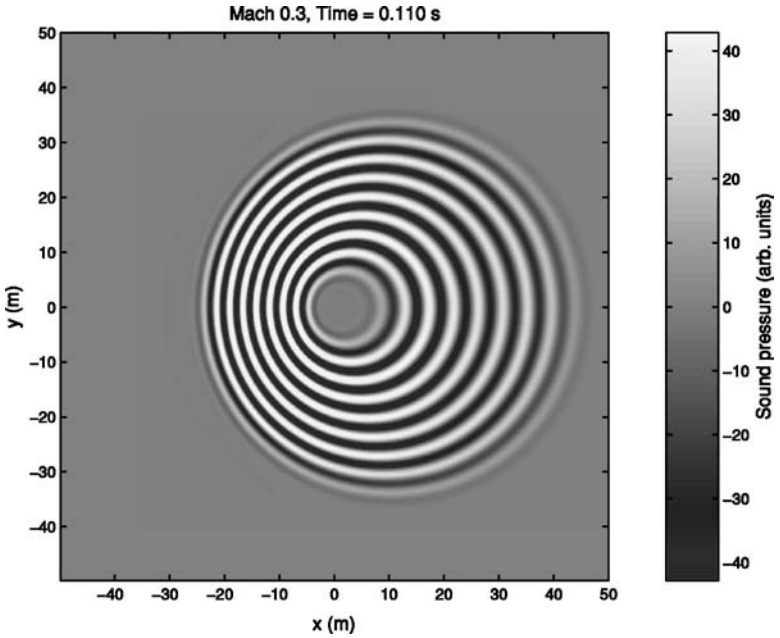

FIG. 3. Wavefronts of the sound pressure due to a point source located at the point $x=0$ and $y=0$ for $M=0.3$. The medium velocity is in the direction of the x-axis.

The methods include the staggered (with forward-differencing of the moving medium terms mentioned in Sec. V B) and nonstaggered leap-frog approaches and the fourth-order Runge–Kutta. The time step for the leap-frog methods was 0.036 ms (1/4 that used for the Runge–Kutta), so that the computational times of all calculations are roughly equal. The Runge–Kutta and nonstaggered leap-frog provide graphically indistinguishable results. The staggered leap-frog, however, systematically underpredicts the amplitude in the downwind direction and overpredicts in the upwind direction. The actual sound pressure signals at $t=0.11$ s, calculated from the staggered and nonstaggered leap-frog approaches, are overlaid in Fig. 5. In the downwind direction, the staggered leap-frog method provides a smooth prediction at distances greater than about 22 m. The noisy appearance at shorter distances is due to numerical instability, which was clear from the rapid temporal growth of these features we observed as the calculation progressed. We conclude that the staggered leap-frog approach, when applied to a moving medium, is less accurate and more prone to numerical instability. This is likely due to the nonsymmetric temporal finite difference approximations for the moving medium terms.

Figure 6 shows the azimuthal dependence of $|p(r,\alpha,M)/p(r,0,0)|$ for $M=0$, 0.3, and 0.6. All FDTD calculations for this figure use the fourth-order Runge–Kutta method. Two calculated curves are shown: one for a low-resolution run with 800×800 grid points and a time step of 0.145 ms, and the other for a high-resolution run with 1600×1600 grid points and a time step of 0.0362 ms. For $M=0.3$, both grid resolutions yield nearly exact agreement with Eq. (72). At $M=0.6$, the low-resolution run has 11 spatial grid nodes per wavelength in the upwind direction and a downwind Courant number of 0.64. The high-resolution grid has 22 spatial grid nodes per wavelength in

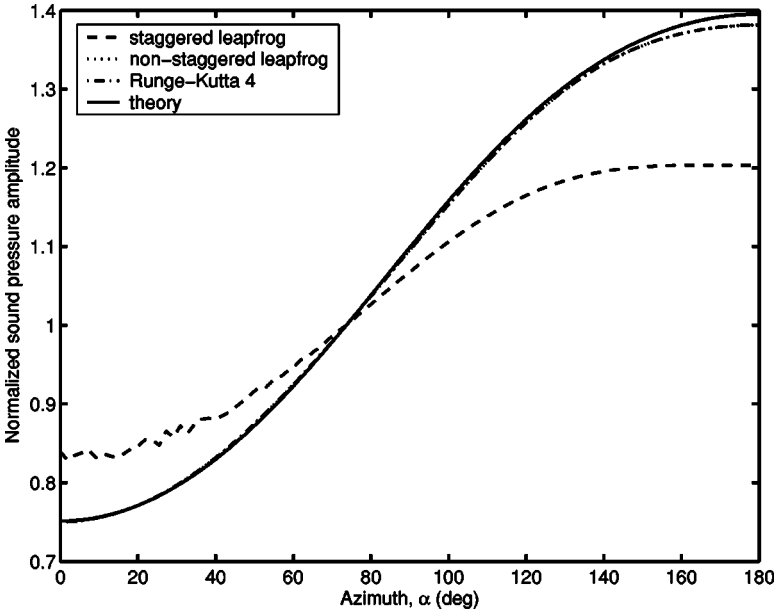

FIG. 4. Normalized sound pressure amplitude $|p(r,\alpha,M)/p(r,0,0)|$ versus the azimuthal angle α for $M=0.3$ and $kr=20$. The staggered and nonstaggered leap-frog methods and the fourth-order Runge–Kutta are compared to the theoretical solution. The nonstaggered leap-frog and Runge–Kutta methods are graphically indistinguishable.

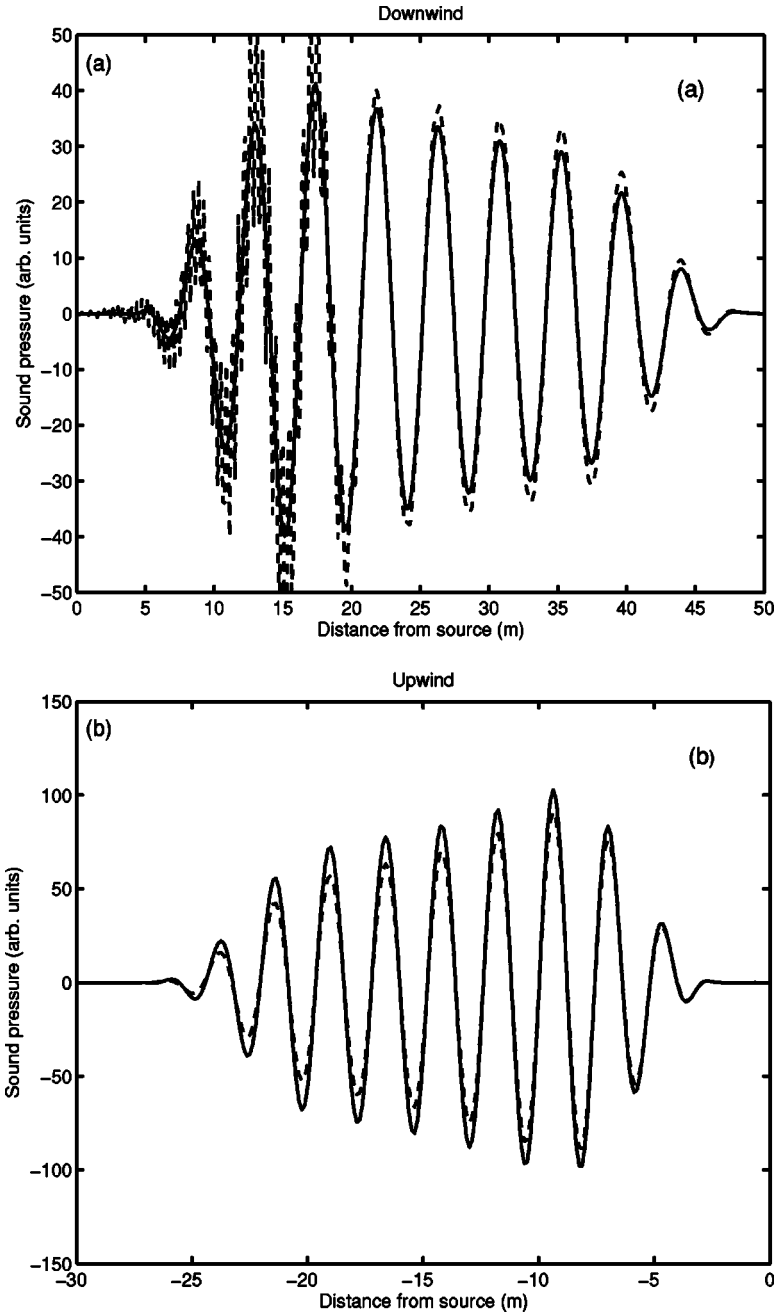

FIG. 5. Sound pressure traces for (a) downwind and (b) upwind propagation. Calculations from the staggered and nonstaggered leap-frog methods are shown (dashed and solid lines, respectively).

the upwind direction and a downwind Courant number of 0.32. Agreement with theory at $M=0.6$ is very good for the high-resolution run. The low-resolution run substantially underpredicts the upwind amplitude.

Finally note that it follows from Figs. 4 and 6 that the sound pressure is largest for $\alpha=180°$, i.e., in the upwind direction. This dependence is also evident upon close examination in Fig. 3.

E. Comparison of FDTD and FFP calculations

The computational examples so far in this paper have been for uniform flows. However, the numerical methods and equations upon which they are based apply to nonuniform flows as well. In this section, we consider an example calculation for a flow with constant shear. The point source and receiver are both located at a height of 20 m and the frequency is 100 Hz. The computational domain is 200 m by 100 m and has 600 by 300 grid points. The time step is 7.73×10^{-4} s and the fourth-order Runge–Kutta method is used. A rigid boundary condition is applied at the ground surface ($y=0$ m). An absorbing layer in the upper one-fifth of the simulation domain removes unwanted numerical reflections. (The implementation of the rigid ground boundary condition and the absorbing layer is described in Ref. 34. Realistic ground boundary conditions in a FDTD simulation of sound propagation in the atmosphere are considered in Ref. 35.)

Calculated transmission loss (sound level relative to free space at 1 m from the source) results are shown in Figs. 7(a) and 7(b). The first of these figures is for a zero-wind condition and the second is for a horizontal (x-direction) wind speed of $v(y)=\mu y$, where the gradient μ is 1 s^{-1}. For Fig.

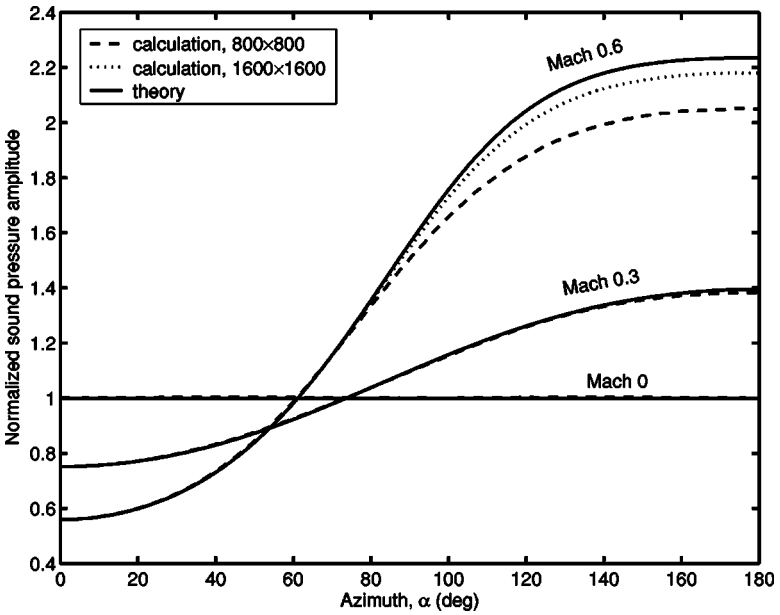

FIG. 6. Normalized sound pressure amplitude $|p(r,\alpha,M)/p(r,0,0)|$ versus the azimuthal angle α for $M=0$, 0.3, and 0.6. The fourth-order Runge–Kutta method was used. The calculation with 800×800 grid points had a spatial resolution of 0.125 m and time step 0.145 ms, whereas the 1600×1600 calculation had a spatial resolution of 0.0625 m and time step 0.0362 ms.

7(a), the FDTD results are compared with both the exact solution for a point source above the rigid boundary and calculations from the FFP developed in Ref. 36. The FDTD results are nearly indistinguishable from the exact solution. The FFP is also in good agreement, although there is some systematic underprediction of the interference minima, particularly so near the source. This is likely due to the far-field approximation inherent to the FFP. For the case with constant shear, Fig. 7(b), the interference pattern is shifted. The FDTD and FFP continue to show very similar small discrepancies near the source. On the basis of the results shown in Fig. 7(a), it is highly likely that the FDTD is more accurate. The FDTD calculations required about 100 times as long to complete as the FFP on a single-processor computer. As would be expected, the FFP is more efficient for calculations at a limited number of frequencies in a horizontally stratified medium.

VI. CONCLUSIONS

In the present paper, we have considered starting equations for FDTD simulations of sound propagation in a moving inhomogeneous atmosphere. FDTD techniques can provide a very accurate description of sound propagation in complex environments.

A most general description of sound propagation in a moving inhomogeneous medium is based on the complete set of linearized equations of fluid dynamics, Eqs. (5)–(8). However, this set is too involved to be effectively employed in FDTD simulations of outdoor sound propagation. In this paper, the linearized equations of fluid dynamics were reduced to two simpler sets of equations which can be used as starting equations for FDTD simulations.

The first set of equations contains three coupled equations, Eqs. (5), (6), and (13), for the sound pressure p, acoustic velocity $\mathbf{w}$, and acoustic density η. This set is an exact consequence of the linearized equations of fluid dynamics, Eqs. (5)–(8). To solve the first set of equations, one needs to know the following ambient quantities: the adiabatic sound speed c, density ϱ, medium velocity $\mathbf{v}$, pressure P, and the parameters α, β, and h. The atmosphere can be modeled as an ideal gas to a very good accuracy. In this case, the first set of equations simplifies and is given by Eqs. (5), (6), and (15). Now it contains the following ambient quantities: c, ϱ, $\mathbf{v}$, and P.

The second set of starting equations for FDTD simulations contains two coupled equations for the sound pressure p and acoustic velocity $\mathbf{w}$, Eqs. (17) and (18). In order to solve this set one needs to know a fewer number of the ambient quantities: c, ϱ, and $\mathbf{v}$. Note that namely these ambient quantities appeared in most of equations for the sound pressure p which have been previously used for analytical and numerical studies of outdoor sound propagation. The second set was derived from Eqs. (5)–(8) assuming that terms proportional to the divergence of the medium velocity and the gradient of the ambient pressure can be ignored. Both these assumptions are reasonable in atmospheric acoustics. To better understand the range of applicability of the second set, it was compared with equations for the sound pressure p which have been most often used for analytical and numerical studies of sound propagation in a moving inhomogeneous medium. It was shown that the second set has the same or wider range of applicability than these equations for p. Thus, a relatively simple set of Eqs. (17) and (18), which is however rather general, seems very attractive as starting equations for FDTD simulations.

The numerical algorithms for FDTD solutions of the second set of equations were developed for the case of a 2-D inhomogeneous moving medium. It was shown that the staggered-in-time grid approach commonly applied to nonmoving media cannot be applied directly for the moving case. However, fairly simple alternatives based on nonstaggered-in-time grids are available. We used the resulting algorithms to calculate the sound pressure due to a point source in a homogeneous uniformly moving medium. The results obtained were found in excellent agreement with analytical predictions even for a Mach number as high as 0.6.

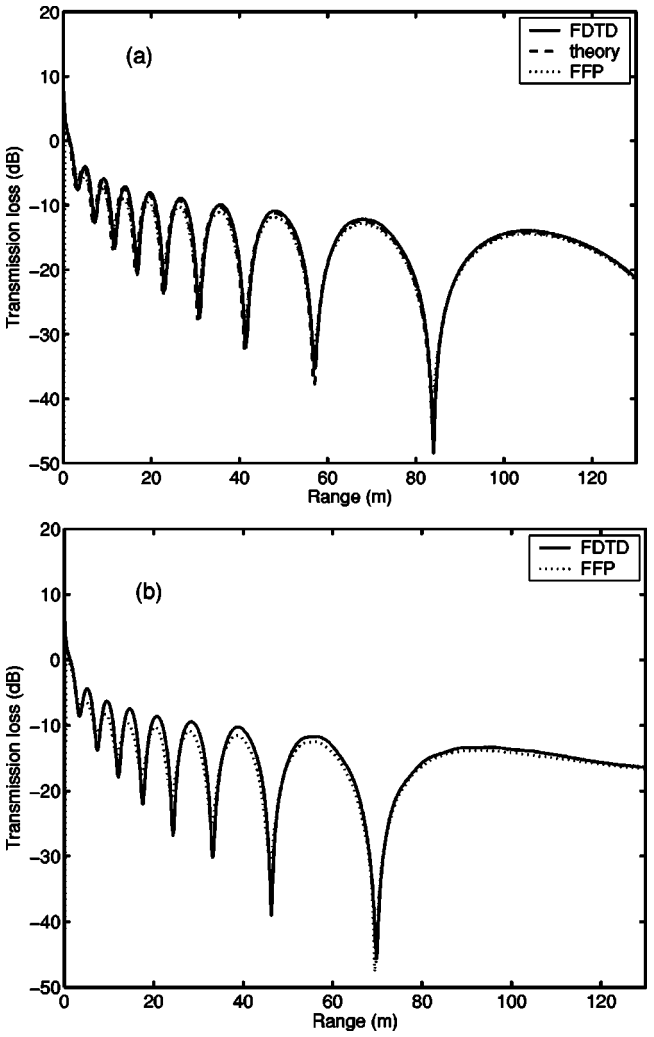

FIG. 7. Comparisons between the transmission loss calculated with different methods. (a) Homogeneous atmosphere without wind. (b) Atmosphere with linearly increasing wind velocity.

Furthermore, using the algorithm developed, we calculated the sound field due to a point source in a stratified moving atmosphere. The results obtained are in a good agreement with the FFP solution.

Finally note that Eqs. (17) and (18) have already been used as starting equations in FDTD simulations of sound propagation in 3-D moving media with realistic velocity fields. The results obtained were published in proceedings of conferences.[5–8] These realistic velocity fields include the following: kinematic turbulence generated by quasi-wavelets,[5,6] 3-D stratified moving atmosphere,[6] and atmospheric turbulence generated by large-eddy simulation.[7] In Ref. 8, FDTD simulations were used to numerically study infrasound propagation in a moving atmosphere over distances of several hundred km. The largest run to date incorporated over 1.5 billion nodes and took about 100 hours on 500 Compaq EV6 parallel processors.[8]

ACKNOWLEDGMENTS

This article is partly based upon work supported by the DoD High-Performance Computing Modernization Office project ''High-Resolution Modeling of Acoustic Wave Propagation in Atmospheric Environments'' and the U.S. Army Research Office Grant No. DAAG19-01-1-0640.

APPENDIX: SOUND FIELD DUE TO A POINT MONOCHROMATIC SOURCE IN A HOMOGENEOUS UNIFORMLY MOVING MEDIUM

In this appendix, we derive a formula for the sound pressure due to a point monochromatic source located in a 2-D homogeneous uniformly moving medium (see Fig. 2).

For this geometry, Eqs. (68) and (69) can be reduced to a single equation for the sound pressure:

$$\left(\frac{\partial}{\partial t}+\mathbf{v}\cdot\boldsymbol{\nabla}\right)^2 p-c^2\nabla^2 p=\varrho c^2\left(\frac{\partial}{\partial t}+\mathbf{v}\cdot\boldsymbol{\nabla}\right)Q. \tag{A1}$$

Here, the source function Q is given by Eq. (70) and contains the time factor $\exp(-i\omega t)$. In what follows, this time factor is omitted. Furthermore, taking into account that the medium velocity is parallel to the x-axis, Eq. (A1) can be written as

$$\left(\frac{\partial^2}{\partial x^2}+\frac{\partial^2}{\partial y^2}+k^2+2ikM\frac{\partial}{\partial x}-M^2\frac{\partial^2}{\partial x^2}\right)p(x,y)$$

$$=\frac{2iA}{\omega}\left(i\omega-v\frac{\partial}{\partial x}\right)\delta(x)\,\delta(y). \tag{A2}$$

Let

$$p(x,y)=\frac{2iA}{\omega}\left(i\omega-v\frac{\partial}{\partial x}\right)\Phi(x,y). \tag{A3}$$

Substituting this formula into Eq. (A2), we obtain the following equation for the function $\Phi(x,y)$:

$$\left[\frac{\partial^2}{\partial x^2}+\frac{\partial^2}{\partial y^2}-\left(-ik+M\frac{\partial}{\partial x}\right)^2\right]\Phi(x,y)=\delta(x)\,\delta(y). \tag{A4}$$

In this equation, let us make the following transformations:

$$x=\sqrt{1-M^2}X,\quad k=\sqrt{1-M^2}K,$$

$$\Phi(x,y)=\exp(-iKMX)\Psi(X,y). \tag{A5}$$

As a result, we obtain the following equation for the fuinction $\Psi(X,y)$:

$$\left[\frac{\partial^2}{\partial X^2}+\frac{\partial^2}{\partial y^2}+K^2\right]\Psi(X,y)=\frac{1}{\sqrt{1-M^2}}\,\delta(X)\,\delta(y). \tag{A6}$$

A solution of this equation is well known:

$$\Psi(X,y)=-\frac{i}{4\sqrt{1-M^2}}H_0^{(1)}(K\sqrt{X^2+y^2}). \tag{A7}$$

Using this expression for Ψ and Eqs. (A3) and (A5), we obtain a desired formula for the sound pressure of a point monochromatic source in a 2-D homogeneous uniformly moving medium:

$$p(x,y)=\frac{iA}{2(1-M^2)^{3/2}}\left[H_0^{(1)}(\xi)-\frac{iMkx}{\xi(1-M^2)}H_1^{(1)}(\xi)\right]$$

$$\times\exp\left(-\frac{ixkM}{1-M^2}\right). \tag{A8}$$

Here, $\xi = (k/\sqrt{1-M^2})\sqrt{x^2/(1-M^2)+y^2}$. In polar coordinates, Eq. (A8) becomes Eq. (71).

[1] R. Blumrich and D. Heinmann, "A linearized Eulerian sound propagation model for studies of complex meteorological effects," J. Acoust. Soc. Am. **112**, 446–455 (2002).

[2] E. M. Salomons, R. Blumrich, and D. Heinmann, "Eulerian time-domain model for sound propagation over a finite-impedance ground surface. Comparison with frequency-domain models," Acust. Acta Acust. **88**, 483–492 (2002).

[3] T. Van Renterghem and D. Botteldoren, "Numerical simulation of the effect of trees on downwind noise barrier performance," Acust. Acta Acust. **89**, 764–778 (2003).

[4] T. Van Renterghem, "The finite-difference time-domain method for simulation of sound propagation in a moving medium," Doctoral thesis, Universiteit Gent, 2003.

[5] D. K. Wilson, M. L. Moran, L. Liu, V. E. Ostashev, D. F. Aldridge, N. P. Symons, and D. H. Marlin, "Development of a high-fidelity simulation capability for battlefield acoustics," in *Proceedings of SPIE AeroSense 2003*, Orlando, FL, 2003.

[6] D. H. Marlin, D. F. Aldridge, N. P. Symons, D. K. Wilson, and V. E. Ostashev, "Finite-difference time-domain acoustic wave propagation in complex atmospheric environments: Second year results," in *Proceedings of the Military Sensing Symposia (MSS) Specialty Group on Battlefield Acoustic and Seismic Sensing, Magnetic and Electric Field Sensors*, Laurel, MD, 2003.

[7] D. K. Wilson, N. P. Symons, E. G. Patton, P. P. Sullivan, D. H. Marlin, D. F. Aldridge, V. E. Ostashev, S. A. Ketcham, E. L. Andreas, and S. L. Collier, "Simulation of sound propagation through high-resolution atmospheric boundary layer turbulence fields," in *Proceedings of the 16th American Meteorological Society Symposium on Boundary Layers and Turbulence*, Portland, ME, 2004.

[8] N. P. Symons, D. F. Aldridge, D. H. Marlin, D. K. Wilson, E. G. Patton, P. P. Sullivan, S. L. Collier, V. E. Ostashev and D. P. Drob, "3D staggered-grid finite-difference simulation of sound refraction and scattering in moving media," in *Proceedings of the 11th International Symposium on Long Range Sound Propagation*, Fairlee, VT, 2004.

[9] V. E. Ostashev, *Acoustics in Moving Inhomogeneous Media* (E&FN SPON, London, 1997).

[10] A. D. Pierce, *Acoustics—An Introduction to its Physical Principles and Applications* (McGraw-Hill, New York, 1989).

[11] L. M. Brekhovskikh and O. A. Godin, *Acoustics of Layered Media* (Springer-Verlag, Berlin, 1992).

[12] M. E. Goldstein, *Aeroacoustics* (McGraw-Hill, New York, 1976).

[13] V. I. Tatarskii, *The Effects of the Turbulent Atmosphere on Wave Propagation* (Israel Program for Scientific Translation, Jerusalem, 1971).

[14] A. D. Pierce, "Wave equation for sound in fluids with unsteady inhomogeneous flow," J. Acoust. Soc. Am. **87**, 2292–2299 (1990).

[15] D. F. Aldridge, "Acoustic wave equations for a linear viscous fluid and an ideal fluid," SAND Report SAND2002-2060, Sandia National Laboratories, Albuquerque, NM, 2002. (Available from the U.S. Dept. of Commerce National Technical Information Service, http://www.ntis.gov/ordering.htm.)

[16] L. D. Landau and E. M. Lifshitz, *Fluid Mechanics* (Pergamon, New York, 1987).

[17] D. I. Blokhintzev, *Acoustics of an Inhomogeneous Moving Medium* (Nauka, Moscow, 1946) (in Russian); (English translation, Department of Physics, Brown Univ., Providence, RI, 1956).

[18] C. K. W. Tam and Y. C. Webb, "Dispersion-relation-preserving finite difference schemes for computational acoustics," J. Comput. Phys. **107**, 262–281 (1993).

[19] C. Bogey, C. Bailly, and D. Juvé, "Computation of flow noise using source terms in linearized Euler's equations," AIAA J. **40**, 235–243 (2002).

[20] C. Bailly, P. Lafon, and S. Candel, "A stochastic approach to compute noise generation and radiation of free turbulent flows," AIAA Paper No. 95-092, 1995.

[21] J. C. Hardin and D. S. Pope, "An acoustic/viscous splitting technique for computational aeroacoustics," Theor. Comput. Fluid Dyn. **6**, 323–340 (1994).

[22] W. Z. Shen and J. N. Sorensen, "Aeroacoustic modeling of low-speed flows," Theor. Comput. Fluid Dyn. **13**, 271–289 (1999).

[23] W. Z. Shen and J. N. Sorensen, "Aeroacoustic modeling of turbulent airfoil flows," AIAA J. **39**, 1057–1064 (2001).

[24] R. Ewert and W. Schroder, "Acoustic perturbation equations based on flow decomposition via source filtering," J. Comput. Phys. **188**, 365–398 (2003).

[25] V. E. Ostashev, "On sound wave propagation in a three-dimensional inhomogeneous moving medium," in *Diffraction and Wave Propagation in Inhomogeneous Media* (MPTI Press, Moscow, 1987), pp. 42–49.

[26] Ph. Blanc-Benon, L. Dallois, and D. Juvé, "Long range sound propagation in a turbulent atmosphere within the parabolic approximation," Acust. Acta Acust. **87**, 659–669 (2001).

[27] K. S. Yee, "Numerical solution of initial boundary value problems involving Maxwell's equations in isotropic media," IEEE Trans. Antennas Propag. **14**, 302–307 (1966).

[28] D. Botteldooren, "Acoustical finite-difference time-domain simulation in a quasi-Cartesian grid," J. Acoust. Soc. Am. **95**, 2313–2319 (1994).

[29] R. W. Graves, "Simulating seismic wave propagation in 3D elastic media using staggered-grid finite differences," Bull. Seismol. Soc. Am. **86**, 1091–1106 (1996).

[30] J. O. A. Robertsson, J. O. Blanch, and W. W. Symnes, "Viscoelastic finite-difference modeling," Geophysics **59**, 1444–1456 (1994).

[31] A. Kasahara, "Computational aspects of numerical models for weather prediction and climate simulation," in *Methods in Computational Physics*, edited by J. Chang (Academic, New York, 1977), pp. 1–66.

[32] E. Kreyszig, *Advanced Engineering Mathematics*, 6th ed. (Wiley, New York, 1988).

[33] L. R. Lines, R. Slawinski, and R. P. Bording, "A recipe for stability of finite-difference wave-equation computations," Geophysics **64**, 967–969 (1999).

[34] D. K. Wilson and L. Liu, "Finite-difference, time-domain simulation of sound propagation in a dynamic atmosphere," Cold Regions Research and Engineering Laboratory Technical Report ERDC-CRREL TR-04-12, Hanover, NH, 2004, p. 63, available from the National Technical Information Center, http://www.ntis.gov/, Technical Report, ADA423222.

[35] S. L. Collier, V. E. Ostashev, D. K. Wilson, and D. H. Marlin, "Implementation of ground boundary conditions in a finite-difference time-domain model of acoustic wave propagation," in *Proceedings of the Military Sensing Symposia (MSS) Specialty Group on Battlefield Acoustic and Seismic Sensing, Magnetic and Electric Field Sensors*, Laurel, MD, 2003.

[36] D. K. Wilson, "Sound field computations in a stratified, moving medium," J. Acoust. Soc. Am. **94**, 400–407 (1993).